Abstract

We report a LEED study of Cu(111) and one monolayer of iron epitaxially grown on Cu(111). A full dynamical analysis was performed using the renormalized forward scattering method. We studied the influence of the scattering potential employed on the quality of the LEED theoretical analysis. We observed that the values of the real part of the inner potential is strongly dependent on the scattering potential used in the calculations. The analysis of the intensity vs energy for all the spots at room temperature gave a 2% contraction for the topmost layer of Cu(111) and 3% contraction for one monolayer of iron (in reference to Cu(111) bulk). We also detected Cu surface segregation at relative low temperatures (473K) for iron epitaxially grown on Cu (111). Time and temperature play a significant role on the surface segregation process. Great care must be exercised when studying the electronic and magnetic properties of epitaxially grown fcc iron on Cu(111) when samples are prepared above room temperature.

INTRODUCTION

The study of the epitaxial growth of 3d-metals on single crystal substrates has been the subject of several theoretical and experimental studies.[1-8] This scientific problem is of considerable importance both for experimental and theoretical reasons. The surface structure determines the reactivity and selectivity of catalysts.[9] Also more recently there has been a great deal of interest on the magnetic properties of iron surfaces epitaxially grown on fcc Cu.[10-13] The mode of growth of the iron film can determine what level of magnetism the surface will show. Island free growth is not always observed in these materials and contradictory reports can be found in the literature concerning the properties of such metal overlayers.

The most valuable technique for the characterization of the surface structure is Low Energy Electron Diffraction (LEED), this technique is unique in giving information on the morphology of the surface as well as on the interplanar spacings.[14] The determination of surface structures involves measuring the intensities of the elastically diffracted beams as a function of the incident electron energy and comparing these with the results of theoretical calculations performed with appropriate models which take into consideration multiple scattering processes.

In the present study we reexamined Cu(111) as a reference point to our main purpose, a LEED characterization of an iron monolayer on Cu(111). The LEED analysis of Cu(111) involves multiple relaxation and temperature dependent effects which to our knowledge has not been reported previously. We also performed a systematic study of the

effect of the type of scattering potential used in the calculations on the quality of the LEED analysis.

In the following paragraphs we discuss the experimental and theoretical procedure, employed for the study of Cu(111) and one monolayer (ML) of iron on Cu(111).

EXPERIMENTAL TECHNIQUES

The iron deposition and measurements were performed in an ultrahigh vacuum system, which has been previously described.[5,6] The substrate was Cu(111) which was previously electropolished and aligned using von Laue X-ray diffraction. Prior to each evaporation, the Cu(111) crystal surface was cleaned by several cycles of Ar ion sputtering and subsequent annealing at 550°C for about 10 min. An occasional oxygen treatment was necessary to remove residual impurities on the Cu(111) surface. The iron metal was evaporated from a Knudsen cell with water cooled electrodes, the cell consisted of an aluminum crucible mounted inside a tantalum furnace. A shutter in front of the cell allowed outgassing and stabilization of the deposition rate to facilitate reproducibility in the evaporation of the metal. The pressure during deposition was in the high 10^{-10} torr range. The samples were prepared with the substrate at room temperature (RT), since we found clear evidence of surface segregation of Cu at higher temperatures, (an often ignored effect). Auger spectra were taken before and after each set of LEED measurements. Auger electron spectroscopy (AES) was also employed to determine the overlayer thickness. A cylindrical mirror analyzer was used for such measurements. The variation in intensity of the 651 eV Fe Auger peak and the

920 eV Cu peak were used to determine the coverage. For low coverage better sensitivity was obtained by monitoring the attenuation of the $M_{2,3}VV$ and M_1VV Auger Transition of Cu as a function of iron coverage. The measurements indicates a layer-by-layer growth up to about 5ML. However, at such high coverages, there is evidence of oxygen and carbon contamination (0.1 of ML). The Fe monolayer didn't show the presence of any C or O impurities within the sensitivity of Auger spectroscopy. No superstructures were observed for coverages less than 5 ML of iron. LEED measurements were performed at RT, 423K, and 523K for clean Cu(111) and RT, 373K and 473K for 1ML of iron on Cu(111). The LEED spots were very well defined and clear, although for temperatures around 473K a broadening of the spots was observed.

LEED intensity-versus-energy curves were obtained by using a spot photometer (Photo Research, Model UBD-1/4). The output voltages from the spot photometer and the beam current from the LEED module were passes through an ADC into an Apple II+ computer. A Varian four-grid LEED system was used in these measurements. Prior to the measurements, adjustments using trimming magnets, Helmhotz coils and φ and θ-rotations were made so that all spots of the same symmetry had equal intensities. Energy scales are given with reference to the vacuum level. The experimental intensity versus energy spectra were recorded for (10), $(\bar{1}1)$, $(0\bar{1})$, (01), $(\bar{1}0)$, $(1\bar{1})$, (11), $(\bar{2}1)$, $(\bar{1}\bar{1})$, $(2\bar{1})$, (20), $(0\bar{2})$, (02) and (00). Figure 1 shows the position of the beams as observed on the LEED screen. The symmetry related beams were averaged to correct for any small misalignment. In order to obtain the I vs. E curves for the (00) beam, the sample was tilted out of the axis of the electron gun. The value of the angles θ and φ could be measured

directly from the photographs of the LEED pattern. In this work we employed the method described by Cunningham and Weinberg[15] to determine φ and θ. In Figure 2 we illustrate the quality of our orientation of the crystal by calculating the reliability factors for two symmetric beams for Cu(111) and 1ML Fe on Cu(111).

EXPERIMENTAL RESULTS AND ANALYSIS

Dynamical model:

The theoretical calculations are based on the dynamical theory of LEED. Our programs are fundamentally based on the model of Van Hove and S.Y. Tong.[16] A muffin-tin geometry is employed in these calculations for the surface and layer potentials. The crystal is divided into layers of identical 2-D symmetry, each layer consisting of a single Bravais lattice. Diffraction from each layer is calculated exactly, reflection and transmission by stacked layers are evaluated using the renormalized forward scattering method. The effect of temperature is included through temperature dependent phase shifts using a Debye-Waller factor. Sixty-one beams and eight phase shifts were employed in our calculations. Increasing the number of phase shifts didn't appreciably change the accuracy of the results, but created a significant increase in computational time. In our calculations the structural and non-structural parameters are varied until a minimum in the reliability factor is obtained. The parameters that are varied in the calculations are:

i) the interlayer spacings (d_{12}, first layer, d_{23} second layer, d_{34} third layer and bulk);

ii) real and imaginary parts of the inner potential;

iii) bulk and surface Debye temperatures; and

iv) scattering potential.

The interlayer spacings were varied independently until a minimum was obtained in the reliability factor. We found that the LEED analysis is less sensitive to variations in the third interlayer spacing, d_{34}, than to d_{12} and d_{23}. The quality of the LEED analysis of the experimental data shows great sensitivity towards variations in d_{23}. The second interlayer spacing shows great variations in value, depending on the number of beams used. It means that if a small number of beams are used one obtains values of d_{23} that show a dependence on the number of beams employed in the calculations. In our model we used a large enough number of beams so that d_{23} becomes independent of the number of beams. The topmost layer, d_{12}, shows a similar dependence, although not as strong as d_{23}.

The real part of the inner potential was varied in the reliability factor program. It was set initially to -10 eV and varied in the range of -20 eV to 0 eV. The imaginary part of the inner potential was varied from -3 eV to -5 eV until an optimum reliability factor was obtained. The bulk and surface Debye temperatures were varied independently until a minimum in the reliability factor was obtained.

In our calculations we tested several scattering potentials in order to test the sensitivity of the LEED analysis to such a parameter. It was found, as mentioned earlier by P.M. Marcus and F. Jona[14], that the quality of the LEED analysis is highly dependent on the accuracy of the scattering potential. Since the electron scattering is mainly dominated by the atom core, the quality of the scattering potential can be improved if a constant potential is added to the

ground state potential (core-shift).[14] The value of this constant potential is obtained by trial until a minimum in the reliability factor is obtained. The better the initial scattering potential, the smaller the value of the added constant potential. In order to get the same quality of LEED analysis one needs a ten times larger core-shift for an atomic potential than the shift needed for a self-consistent potential. One can in principle obtain accurate LEED analysis using core-shifts applied to atomic potentials, in particular when no self consistent potentials are available. The inner potential (real part) and the second interlayer spacing are found to be very sensitive to the type of scattering potential employed in the calculations. The sensitivity of the inner potential to variations in the scattering potential was also observed by Watson et al.[17] They performed a LEED analysis for Rh(100) for two different scattering potentials as a result of such analysis they obtained a difference in inner potential of 6 eV between the two cases.

In our analysis we performed LEED calculations using five different potentials.

I) A self-consistent potential (SC) from full potential LMTO (linearized muffin tin orbital) calculations.

II) A self-consistent potential from full potential LMTO calculations without the exchange and correlation effects.

III) A non-self consistent muffin-tin potential.

IV) Atomic potential.

V) Burdick potential (non-self consistent potential).

These five potentials will be employed in discussing the analysis of LEED measurements on Cu(111).

Cu(111):

In this section the LEED intensity vs. energy measurements are compared with our dynamical calculations. The goodness of the agreement is evaluated using the Zanazzi and Jona[18] reliability factor.

In the dynamical calculations we used a lattice constant value of 3.615A for copper. The value of d_{12} and d_{23} varied between 1.96 and 2.16A. The bulk Debye temperature was varied between 300 and 380K, and the surface Debye temperature was varied between 244 and 344K. The optimum values of the Debye's temperatures obtained were 344K and 292K for bulk and surface respectively. A comparison of the quality of the LEED scattering potentials was performed after fixing the values of the Debye temperatures and the imaginary part of the inner potential (-4 eV). The dynamical calculations were performed by varying the interlayer spacings independently (d_{12}, d_{23}) and the real part of the inner potential. Figure 3 shows the best agreements between the dynamical calculations from different scattering potentials and the experimental results for the (00), (10), (01), (11) and (20) beams. From top to bottom the best results of the analysis are given in Table I. In all of the calculations we have assumed a bulk interlayer spacing of 2.0858A. In Figure 3 we also show the dependence of the inner potential value obtained from the dynamical analysis on the type of scattering potential selected. One can also observe by comparing the shifted self-consistent potential and non-shifted self-consistent potential how the quality of the agreement with the experiment can be improved by adding a constant potential to the ground state potential. It is evident from the results that comparable quality in the agreement between the

experiment and the dynamical calculations can be obtained for a shifted atomic potential as well a self-consistent potential.

In general, we find that the potential with exchange and correlation subtracted does worse than the other potentials, particularly at low energies. But the quality of the high energy peaks and the accurate value of the inner potential for this curve suggest that including the proper energy dependence of the exchange correlation potential in a self-consistent potential could provide good results without further modification (core-shift).

Figure 4 shows the experimental LEED measurements and LEED analysis using a shifted muffin-tin potential (non self consistent) with different interlayer spacings. The best agreement between experiment and theory was obtained for d_{12} = 2.04 $\pm$ 0.02A, d_{23} = 2.06 $\pm$ 0.02A and d_{34} = 2.0858A and V_o = -9 eV, the reliability factor value was 0.03. This value of the reliability factor is considered to be a sign of very good agreement. Figure 5 shows the variation of the reliability factor as a function of d_{12} and d_{23} for the above measurements.

We investigated the effect of temperature on the LEED measurements on Cu(111). Figure 6 shows the results for the (00), (10) and (01) beams at 423 and 523K. The analysis was performed using a shifted muffin tin potential. We kept all the parameters at the room temperature values, except for d_{12} and d_{23}. The best agreement between experiment and theory was obtained for a 1% expansion of the topmost layer with no appreciable change in d_{23}. The reliability factors obtained were 0.032 (423K) and 0.04 (523K). This good agreement is a good indication that the values for the Debye temperatures

obtained can reasonably describe the temperature dependence of the LEED intensities for Cu(111).

1ML Fe on Cu(111):

The LEED measurements were performed as in the case of Cu(111), normal incidence was used for the (10), (01), (11), (02) and (20) beams. The peak positions and intensities of the I-E curves for the iron monolayer on Cu(111), remain consistent with an fcc lattice of iron epitaxially grown on Cu(111). The theoretical calculations for 1ML Fe on Cu(111) were performed using the same procedures as for clean Cu(111). The Fe atoms were placed on the Cu(111) lattice points and the interlayer spacings d_{12}, d_{23}, and d_{34} were varied independently. The best value obtained for the surface Debye temperature of iron was 344 $\pm$ 20K. The high value of the Debye temperature is characteristic of fcc iron.[6]

Figure 7 shows the results for 1 ML Fe for various interlayer spacings. A value of -4 eV for the imaginary part of the inner potential was found to give the best agreement with the experiments. The best values for the interlayer spacings, Debye temperature and real part of the inner potential are given in Table II. One monolayer of iron on Cu(111) show a significant contraction of the interlayer spacing as compared to Cu(111). A larger surface Debye temperature and inner potential are also observed for 1 ML FE. Figure 8 shows the variation of the reliability as a function of d_{12} and d_{23}, and as a function of d_{12} and the surface Debye temperature.

We performed temperature dependent LEED measurements on 1 ML of Fe on Cu(111). We observed around 473K over a period of time (1/2

hour or more) evidence of surface segregation of copper. Figure 9 shows the experimental data for the (01) and (10) beams for Cu(111) and 1 ML of Fe. The LEED features of Fe on Cu(111) starts to disappear around 473K and start to look like clean Cu(111). This phenomenon was independently corroborated by performing a careful Auger study as a function of time and temperature. Figure 10 illustrates the result of such measurements.

It is clear that even for a system like Fe/Cu where no alloying occur, surface segregation can be present at relatively low temperatures. This surface segregation of Cu can have significant importance in drawing conclusions about electronic and magnetic properties of fcc iron epitaxially grown on Cu(111).

CONCLUSIONS

We have shown that accurate dynamical calculations can be performed if one uses a shifted atomic potential. We observed that the value obtained for the real part of the inner potential is strongly dependent on the type of scattering potential used in the calculations. We observed that the topmost layer of Cu(111) contracts 2% in reference to the bulk value, there is also a minor contraction of the second interlayer spacings of about 1%. For 1 ML Fe on Cu(111) the contraction of the topmost layer is 3% (in reference to Cu(111) bulk), the second interlayer spacing contracts by about 1% and the third interlayer spacings remains at the same value as bulk Cu(111). We observed clear evidence of Cu surface segregation at 473K for 1 ML Fe epitaxially grown on Cu(111). The observed effect can have serious implications in the analysis of results obtained for iron fcc

epitaxially grown on Cu(111) at high temperatures since it is evident that the surface will not consist of pure iron. Great care must be taken when conclusions are drawn on samples performed above room temperatures. Time and temperature seems to play a significant role on the surface segregation processes for fcc iron grown on Cu(111).

ACKNOWLEDGEMENTS

The authors acknowledge helpful discussions with David Price and B.R. Cooper. This work was supported by the U.S. Department of Energy and West Virginia University Energy Research Center.

References

1. A. Chambers and D.C. Jackson, Phil. Mag. 31, 1357 (1975).
2. I. Abbate, L. Braicovich, and A. Fasan, Phil. Mag. B44, 327 (1981).
3. P.A. Montano, P.P. Vaishnava, and E. Boling, Surf. Sci. 130, 191 (1983).
4. S.P. Tear and K. Roll, J. Phys. C: Solid State Phys. 15, 5521 (1982).
5. M. Abu-Joudeh, P.P. Vaishnava and P.A. Montano, J. Phys. C. Solid State Phys. 17, 6899 (1984).
6. Y. Darici, J. Marcano, H. Min and P.A. Montano, Surf. Sci. 182, 477 (1987).
7. Z.Q. Wang, Y.S. Li, F. Jona and P.M. Marcus (to be published).
8. P.M. Marcus, V.L. Moruzzi, Z.Q. Want, Y.S. Li and F. Jona, Surf. Sci. (in press).
9. J.H. Sinfelt, Surf. Sci. 195, 641 (1977).
10. W. Kummerle and U. Gradmann, Phys. Status Solidi (a) 45, 171 (1978).
11. W. Becker, H.D. Pfannes, and W. Keune, J. Magn. Mater. 35, 53 (1983).
12. C. Rau, C. Schneider, G. Xing, and K. Jamison, Phys. Rev. Lett. 57, 3221 (1986).
13. G. W. Fernando, Y.C. Lee, P.A. Montano, B.R. Cooper, E.R. Moog, H.M. Naik, and S.D. Bader, J. Vac. Soc. (in press).
14. P.M. Marcus and F. Jona, Applications of Surface Science 11/12, 20, (1982).

15. S.L. Cunningham and W. Henry Weinberg, Rev. Sci. Instr. 49, 752 (1978).

16. M.A. Van Hove and S.Y. Tong "Surface Crystallography by LEED", Berlin, Springer Verlag (1979).

17. P.R. Watson, F.R. Shepherd, O.C. Frost and K.A.R. Mitchell, Surf. Sci. 72, 562 (1978).

18. E. Zanazzi and F. Jona, Surf. Sci. 62, 61 (1977).

TABLE I

Comparison of the LEED results obtained by varying the scattering potential employed in the dynamical calculations.

	d_{12}[A]	d_{23}[A]	$-V_o$[eV]	R
Self-consistent potential (SC1)	2.06	2.08	5	0.033
Shifted self-consistent potential (SC2)	2.04	2.06	8	0.032
Shifted atomic potential (AT˙POT)	2.04	2.06	9	0.032
SC potential without exchange and correlation terms (SC-EXC-CORR)	2.06	2.06	8	0.035
Shifted Burdick potential (BURDICK)	2.06	2.08	5	0.038

V_o = Real part of the inner potential

R = Zanazzi and Jona reliability factor

TABLE II

Interlayer spacings, surface Debye temperatures, inner-potential, and reliability factors for Cu(111) and 1 ML Fe on Cu(111) at room temperature.

	d_{12}(A)	d_{23}(A)	d_{34}(A)	θ_D[K]	$-V_0$[eV]	R
Cu(111)	2.04(2)	2.06(2)	d.08(2)	292(20)	9	0.03
1 ML Fe	2.02(2)	2.06(2)	2.08(2)	344(20)	11	0.035

V_o = real part of the inner potential

R = Zanazzi and Jona reliability factor (error in parenthesis)

Figure Captions

Figure 1. This figure indicates the positions of the beams for Cu(111) and the notation employed in identifying the symmetrical beams.

Figure 2. Comparison between two symmetry related experimental beams for a) Cu(111) and b) 1 ML Fe/Cu(111). R is the Zanazzi and Jona reliability factor.

Figure 3. Intensity vs Energy (I-E) curves for the (00), (10), (11) and (20) beams: (SC1)-Self consistent potential; (SC2)-shifted self-consistent potential; (AT.POT)-shifted atomic potential; (SC-EXC-CORR)-self-consistent potential without the exchange and correlation terms; (BURDICK)-shifted Burdick potential.

Figure 4. I-E curves for the (00), (10), (01), (11), and (20) beams of Cu(111). The top curves are the experimental results for the (00) beam ($\theta=5^{o}$, $\phi=56^{o}$)

(A) d_{12}=2.04 A d_{23}=2.06 A

(B) d_{12}=2.04 A d_{23}=2.00 A

(C) d_{12}=2.04 A d_{23}=2.12 A

(D) d_{12}=1.98 A d_{23}=2.06 A

(E) d_{12}=2.10 A d_{23}=2.06 A

Figure 5. Reliability factor vs d_{12} and d_{23} for Cu(111) at room temperature.

Figure 6. I-E curves for the (00), (10), (01) beams of Cu(111) at

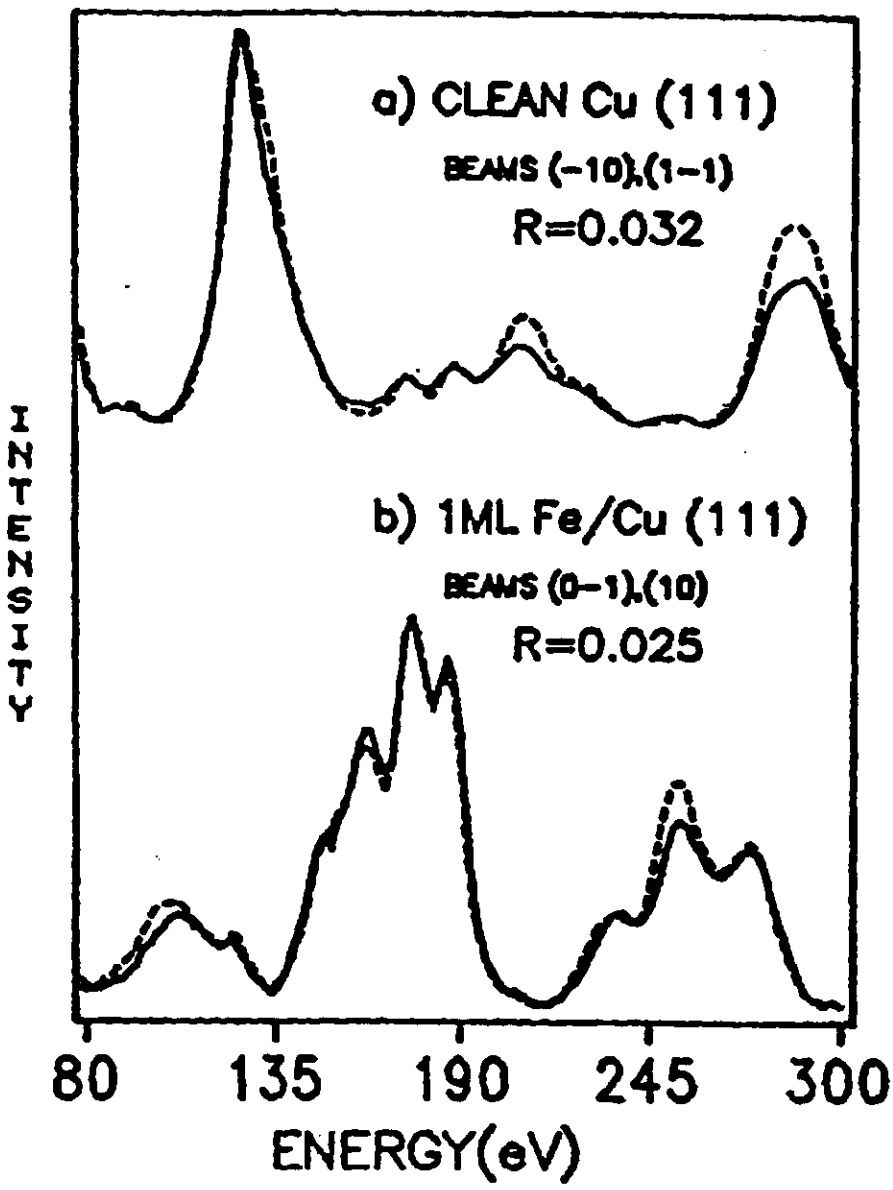
a) CLEAN Cu (111)
BEAMS (-10),(1-1)
R=0.032
b) 1ML Fe/Cu (111)
BEAMS (0-1),(10)
R=0.025
INTENSITY
80
135
190
245
300
ENERGY(eV)

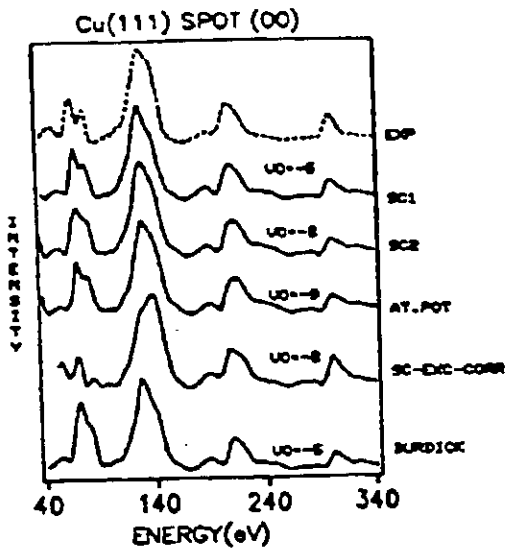
Cu(111) SPOT (00)
IDP
SC1
SC2
AT.POT
SC-EXC-CORR
BURDICK
40
140
240
340
ENERGY(eV)

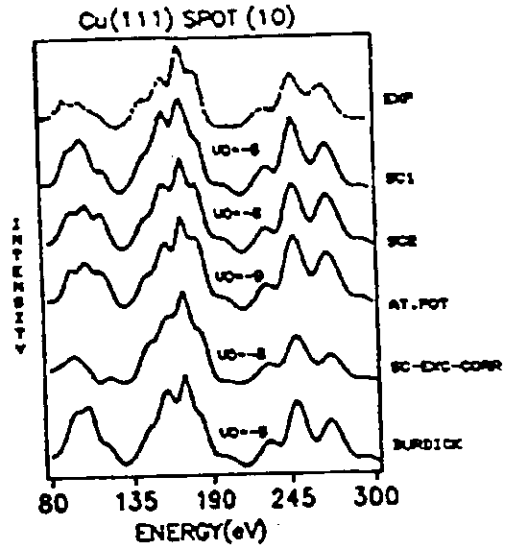
Cu(111) SPOT (10)
IDP
SC1
SC2
AT.POT
SC-EXC-CORR
BURDICK
80
135
190
245
300
ENERGY(eV)

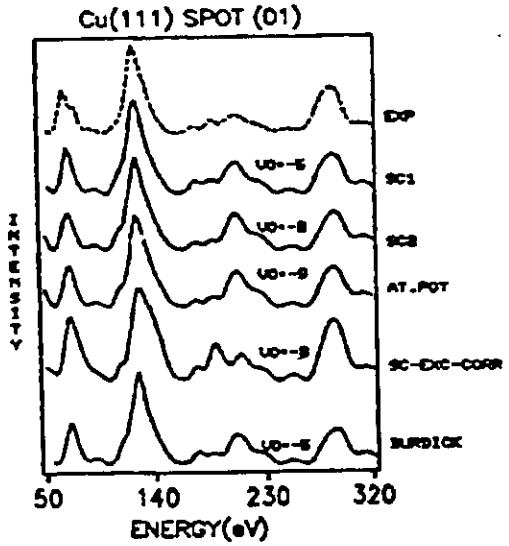
Cu(111) SPOT (01)
IDP
SC1
SC2
AT.POT
SC-EXC-CORR
BURDICK
50
140
230
320
ENERGY(eV)

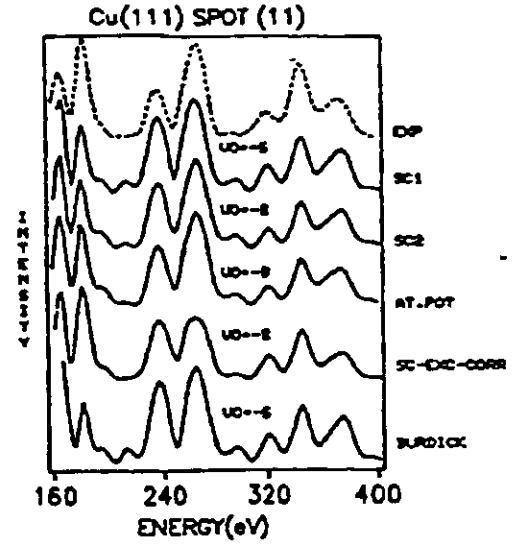
Cu(111) SPOT (11)
IDP
SC1
SC2
AT.POT
SC-EXC-CORR
BURDICK
160
240
320
400
ENERGY(eV)

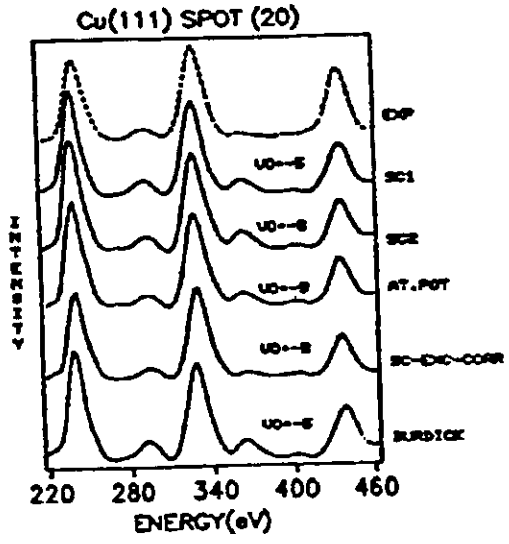
Cu(111) SPOT (20)
IDP
SC1
SC2
AT.POT
SC-EXC-CORR
BURDICK
220
280
340
400
460
ENERGY(eV)

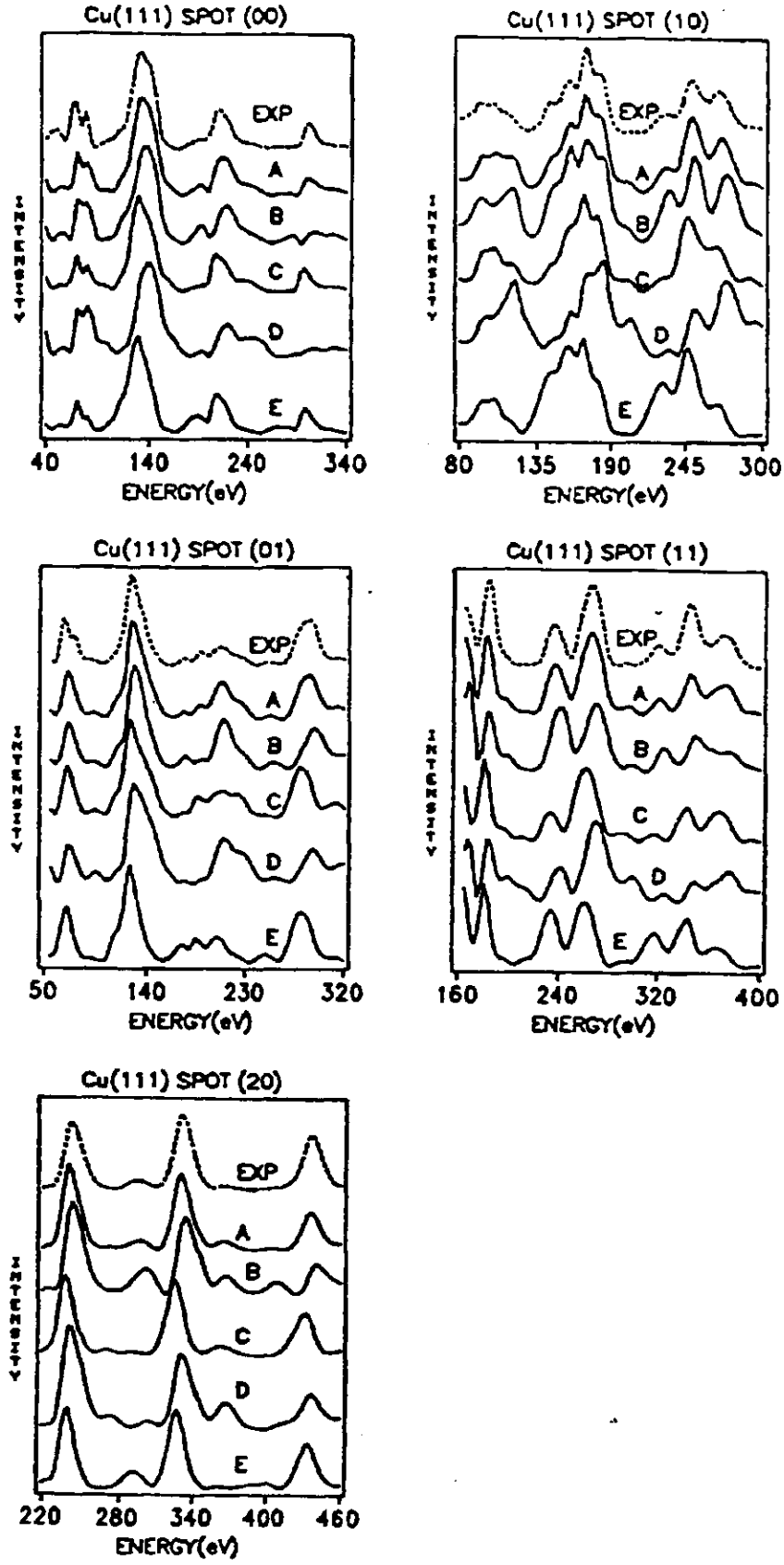
Cu(111) SPOT (00)
EXP
A
B
C
D
E
40
140
240
340
ENERGY(eV)
Cu(111) SPOT (10)
EXP
A
B
C
D
E
80
135
190
245
300
ENERGY(eV)
Cu(111) SPOT (01)
EXP
A
B
C
D
E
50
140
230
320
ENERGY(eV)
Cu(111) SPOT (11)
EXP
A
B
C
D
E
160
240
320
400
ENERGY(eV)
Cu(111) SPOT (20)
EXP
A
B
C
D
E
220
280
340
400
460
ENERGY(eV)